Neutrosophic Control Chart for Rayleigh Quality with Applications To Wind Speed Data

Fuad S. Alduais[1, 2*], Zahid Khan[3], Muhammad Waseem[3]

[1] Mathematics Department, College of Humanities and Science in Al Aflaj, Prince Sattam Bin Abdulaziz University, Al-Kharj, Saudi Arabia
[2] Business Administration Department, Administrative Science College, Thamar University, Thamar, Yemen
[3] Department of Mathematics and Statistics, Hazara University Mansehra Pakistan

Emails: f.alduais@psau.edu.sa; zahidkhan@hu.edu.pk; mwaseem.aziz@gmail.com

Abstract

The application of neutrosophic statistics provides a novel approach to dealing with uncertain and imprecise data problems. In this study, we present an improved method called neutrosophic Rayleigh exponential weighted moving average ($REWMA_N$) chart. The $REWMA_N$ chart is an extension of the traditional V_{NR} model and can be applied in various fields. The proposed $REWMA_N$ scheme is designed to enhance the detection capability of the traditional V_{NR} chart. The key features of the suggested chart are discussed, highlighting its capability to handle vague, indeterminate, and fuzzy data situations. We evaluate the performance of the proposed scheme by analyzing the designated limits and charting parameters for different sample sizes. Moreover, we establish the performance metrics of the $REWMA_N$ chart such as neutrosophic run length (ARL_N) and neutrosophic power curve (PC_N).Performance metrics demonstrate that the $REWMA_N$ chart is highly sensitive to persistent shifts in the scaling parameter of the neutrosophic Rayleigh distribution. Monte Carlo simulations are conducted to compare the suggested scheme with the existing model. A comparative study indicates that the proposed chart outperforms the competing design, particularly in detecting smaller shifts. Finally, we provide a charting structure for the proposed design using daily average wind speed data, which can be used as a practical implementation guideline for real-world applications.

Keywords: Neutrosophic probability; Rayleigh model; Control process; Non-normal quality; Estimation; Simulation

1. Introduction

In the production industry, variability is an inevitable aspect of the manufacturing process and can be attributed to specific causes of variation [1]. Quality management employs several management and technical techniques that remove anomalous variations in order to produce high-quality products [2]. A popular approach called statistical process control (SPC) uses statistical techniques to precisely quantify fluctuations in the parameters of the manufacturing unit [3]. Quality control charts, a very successful SPC tool, are frequently used in the service and industrial sectors to examine process behavior and boost efficiency. Many control chart types exist, and their main purpose is to quickly spot manufacturing abnormalities so that the process may be stopped before incorrect goods are made [4]. The Shewhart chart, established by Walter A. Shewhart, is one of the most widely used control charts [5]. The Shewhart charts are simple to use and understand. Still,

Doi: https://doi.org/10.54216/IJNS.230105
Received: October 05, 2023 Revised: November 01, 2023 Accepted: November 13, 2023

they might not be appropriate for modern processes or service sectors where even little process modifications can have a big financial impact [6].

Memory-type charts, including the MA chart, EWMA chart, and CUSUM chart, have been created to overcome this restriction [7]. Due to the fact that the plotting statistics of these charts take into account both historical data and current data, they are more sensitive to small-to-moderate changes in the target parameters [8]. Conventional control chart design makes the premise that the underlying processes are normal, however, for real-world quality operations, this assumption could not be accurate [9]. Traditional approaches to chart development may not be suitable for non-normal processes and may result in erroneous conclusions [10]. Non-normality-based monitoring techniques have so lately attracted study attention [11]. Other related studies, for instance, Derya and Canan [12] assumed that the observed variable follows the lognormal, Weibull, and gamma distributions in order to devise a monitoring method. Santiago and Smith [13] offered a t-chart based on an exponential distribution, while Rosaiah et al. [14] used the Gumbel distribution to create a charting layout based on percentiles. Hossain, Omar, and Riaz [15] developed the V chart for Maxwell quality parameters, and Guo and Wang [16] and Wang, Bizuneh, and Cheng [17] proposed Weibull model charting designs for full and type II censored data, respectively. The Rayleigh distribution has also been utilized as a valid model for industrial variables [18]-[20].

All of the research above assumes that the parameters of the distribution being used as a quality model are well-defined. However, uncertainty is frequently present in real-world systems and can appear in SPC applications [21]. Control charts cannot accurately explain the process when there is uncertainty in the system, even if human perception depicts the quality attributes [22]. Fuzzy set theory is frequently used to describe and simulate such issues in order to overcome this difficulty [23]. In general, fuzzy control charts are more responsive than traditional control charts [24]. The ideas of fuzzy and classical sets are both expanded upon by the concept of neutrosophic set (NS) [25]. It takes into account the possibility of true, false, and ambiguous circumstances [26]. The concept of the neutrosophic set has been used in several academic disciplines, including SPC [27]. The obtained data may be ambiguous in a number of real-world scenarios, and neutrosophic statistics (NST) is utilized to manage such hazy information on quality features [28]-[32]. Several academics have lately established statistical approaches that are combined with neutrosophic logic in the literature of SPC. Initially, Aslam and Raza [33] developed a sampling approach for several manufacturing lines that used the NST in their investigation. Aslam and Raza [33] and Shafqat et al. [34] provided more information on incorporating the NST into the Shewhart-type chart. Widely used control charts might not be wise when the normality assumption does not flagrantly hold. A statistical distribution that is frequently employed in engineering-related issues and has drawn interest from many scholars is the Rayleigh distribution (RD). One such design that may account for non-normality circumstances for quality data provided by the traditional Rayleigh model is the V_{SQR} design [20]. The dissertation by Khan et al. [21] re-evaluated the V_{SQR} chart and developed the V_{NR} design, which includes a neutrosophic extension of the Rayleigh model. The V_{NR} design is capable of handling uncertain observations of quality characteristics that follow a Rayleigh distribution [21].

This study presents an improved monitoring scheme for the V_{NR} chart, a visual tool for SPC that enables quick response to minute changes in the studied parameter. The suggested chart is an extension of the traditional V_{NR} and is based on the neutrosophic Rayleigh distribution.

The remaining sections of the research are as follows: Preliminaries are discussed in Section 2, the suggested control chart and other important aspects of the proposed model are presented in Section 3, the performance evaluation of the suggested chart is discussed in Section 4, how to generate simulated data and implement the proposed chart are covered in Section 5, a comparison of the proposed chart to existing designs is presented in Section 6, an illustrative example of the proposed chart is given in Section 7, and the results and conclusions are discussed in Section 8.

2. Preliminaries

Let CDF_N be the distribution function of the random variable Y, and let PDF_Nbe the probability density function of random variable Y defined over the range $[0,\infty)$ then the distribution model of the RM_N can be characterized as:

Doi: https://doi.org/10.54216/IJNS.230105
Received: October 05, 2023 Revised: November 01, 2023 Accepted: November 13, 2023

$$\mathrm{CDF_N}(y,\beta_N) = 1 - e^{-\frac{1}{2}\left(\frac{y}{\beta_N}\right)^2};\ \beta_N > 0,\ y > 0. \quad (1)$$

$$\mathrm{PDF_N}(y,\beta_N) = \frac{z}{{\beta_N}^2} e^{-\frac{1}{2}\left(\frac{y}{\beta_N}\right)^2};\ \beta_N > 0,\ y > 0. \quad (2)$$

where$\beta_N \in [\beta_l, \beta_u]$is an imprecise neutrosophic parameter of the $\mathrm{RM_N}$.

In the neutrosophic framework, the mean and variance of the $\mathrm{RM_N}$ respectively can be defined as [25]:

$$\left.\begin{aligned} \mu_N &= \beta_N\sqrt{\frac{\pi}{2}} \\ {\sigma^2}_N &= \frac{4-\pi}{2}{\beta_N}^2 \end{aligned}\right\} \quad (3)$$

Figure 1 illustrates the graphical representations of $\mathrm{CDF_N}$ and $\mathrm{PDF_N}$ for the neutrosophic Rayleigh variable Y with an imprecise parameter of β_N=[1, 2.5].

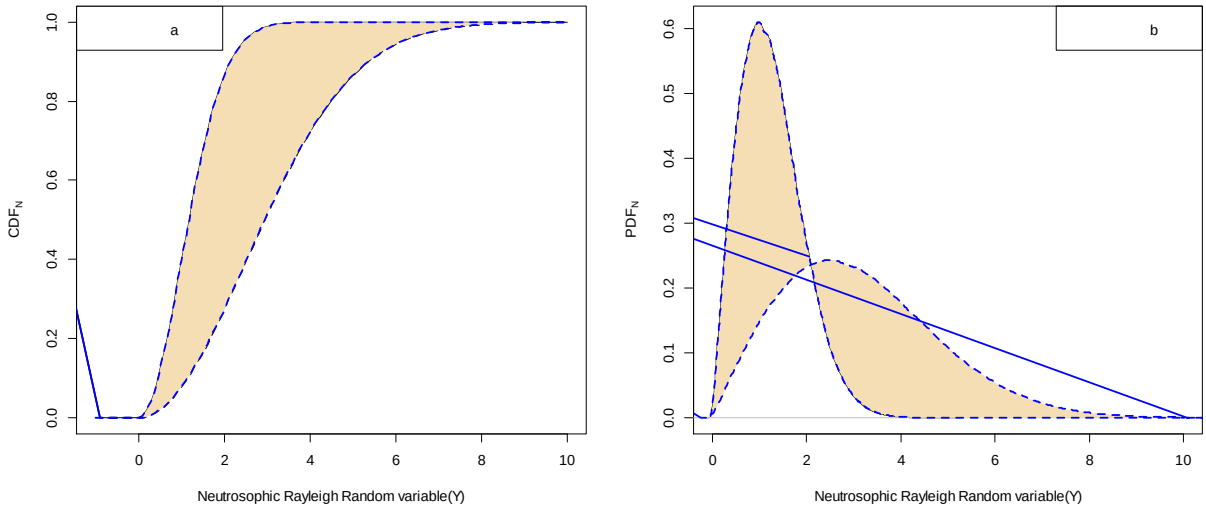

Figure 1: Basic plots of the $\mathrm{CDF_N}$ and $\mathrm{PDF_N}$ of the Rayleigh model with neutrosophic parameter β_N=[1, 2.5].

The chosen values of β_N in Figure 1(a) demonstrate the common non-decreasing behavior of the underlying cumulative distribution function $\mathrm{CDF_N}$, which is a basic property of every distribution function.On the other hand, the neutrosophic zone is depicted as a darkened region between the dotted lines in Figure 1(a). For an arbitrary value of the scale parameter β_N between [1, 2.5], the curve is asymmetric. Due to the impact of the neutrosophic scale parameter, the density function $\mathrm{PDF_N}$ can adopt an infinite variety of structures. A large amount of β_N, however, may produce a symmetric curve.

Based on the expression (3) and the given value of $\beta_N = [1, 2.5]$, computed values of mean and variance are given by:

$\mu_N = [1.25,\ 3.13]$ and ${\sigma^2}_N = [0.429,\ 2.68]$.

In most situations, it is impossible to determine the value of the characterized neutrosophic scale parameter β_N. Various techniques can be utilized to approximate the unknown quantity. The

Doi: https://doi.org/10.54216/IJNS.230105
Received: October 05, 2023 Revised: November 01, 2023 Accepted: November 13, 2023

maximal likelihood (ML) strategy provides an estimate of β_N, as described by Kundu and Raqab [35]:

$$\hat{\beta}_N = \sqrt{\frac{\sum_{i=1}^{n} {y_{iN}}^2}{2n}} \tag{4}$$

where nis neutrosophic sample size is represented by the formula $n = [n_l, n_u]$, and it is equivalent to the classical sample size n when both n_l and n_u are equal to n.

In V_N-chart, statisticβ_N is related to the neutrosophic chi random variable U in the following way [25]:

$$\hat{\beta}_N = \frac{\beta_N}{\sqrt{2\tilde{m}}} U \tag{5}$$

We can determine the mean and variance of the desired statistic $\hat{\beta}_N$ by utilizing the pivotal quantity given in (5) as follows:

$$\left.\begin{aligned} E(\hat{\beta}_N) &= \beta_N H_N \\ Var(\hat{\beta}_N) &= {\beta_N}^2 [1 - H_{N_N}] \end{aligned}\right\} \tag{6}$$

where $H_N = \frac{1}{\sqrt{n}} \frac{\Gamma\left(n+\frac{1}{2}\right)}{\Gamma(n)}$ is neutrosophic constant, and it is the function of a neutrosophic sample size.

Below are the established l-sigma limits for the V_N-chart, which are based on the sampling distribution of the square root statistic.

$$\left.\begin{aligned} LCL_N &= \beta_N H_N - l\beta_N \sqrt{1 - {H_N}^2} \\ UCL_N &= \beta_N H_N + l\beta_N \sqrt{1 - {H_N}^2} \end{aligned}\right\} \tag{7}$$

where LCL_N is a minimum value of the uncertain interval $[LCL_l, LCL_u]$ and UCL_N is the maximum value of the interval $[UCL_l, UCL_u]$ and l is the quantile of the neutrosophic chi-distribution, chosen based on the false alarm rate threshold. The section that follows describes the proposed$REWMA_N$ charting procedure, which is intended to enhance the out-of-control performance of the V_N-chart under conditions of smaller to moderate parameter shifts in the target parameter.

3. Proposed Chart

This section contains the proposed EWMA chat based on the neutrosophic Rayleigh model. Let the random samples$y_{1j}, y_{2j}, \ldots y_{nj}$; (j: 1, 2, 3 ...) of independent and identically distributed realizations of size n betaken at regular interval intervals from the $RM_N$with parameter β_N.The objective is to identify any deviation of β_N from the in-control (IC) value β_{N0}.

The EWMA scheme at time j for calculating the geometric moving average based on the desired statistics can be defined as follows:

$$T_i = (1 - \tau)T_{i-1} + \tau\beta_{Ni} \tag{8}$$

where τ is the crisp smoothing constant that belongs to interval zero and 1, i.e., $0 < \tau \leq 1$ andβ_{Ni} is ith sample computed value of maximum likelihood statistic.

The initial value T_0 is typically set equal to the process target, and the smoothing constant τ decreases, following a geometric progression. When τ equals to 1, the EWMA statistic becomes equal to the latest sample β_N statistic, which is the same as the Shewhart type neutrosophicV_{NR} chart.In this way, the proposed $REWMA_N$ chart represents the general structure.

Using the properties of geometric expansion, the expression (8) can further be written as:

$$T_i = (1 - \tau)^i T_0 + \sum_{j=0}^{i-1} \tau(1 - \tau)^j \beta_{N(i-j)} \tag{9}$$

where $T_0 = \beta_{N0}$ is IC value of the monitoring process.

Doi: https://doi.org/10.54216/IJNS.230105
Received: October 05, 2023 Revised: November 01, 2023 Accepted: November 13, 2023

Due to the smoothing mechanism, the impact of a value on the test statistic diminishes exponentially over time i.e., the impact of $\tau(1-\tau)^j$ quantity decreases exponentially as realizations become less recent. Thus the $REWMA_N$ chart signals if T_i exceed the following lower and upper bounds:

$$\left.\begin{aligned} LCL &= \beta_N H_N - K_N\beta_N\sqrt{1-H_N{}^2}\sqrt{\left(\frac{\tau}{2-\tau}\right)\left[1-(1-\tau)^{2i}\right]} \\ UCL &= \beta_N H_N + K_N\beta_N\sqrt{1-H_N{}^2}\sqrt{\left(\frac{\tau}{2-\tau}\right)\left[1-(1-\tau)^{2i}\right]} \end{aligned}\right\} \quad (10)$$

where $K_N = [K_l, K_u]$ is selected to achieve a desired IC performance or adjustable according to set value of neutrosophic false alarm rate of the proposed chart.

The limits in (11) are known as time-varying limits and usually where the component $(1-\tau)^{2i}$ appraoches to zero as time i increases. Thus the asymptotic form of (10) can be written as:

$$\left.\begin{aligned} LCL &= \beta_N H_N - K_N\beta_N\sqrt{\left(\frac{\tau}{2-\tau}\right)\left(1-H_N{}^2\right)} \\ UCL &= \beta_N H_N + K_N\beta_N\sqrt{\left(\frac{\tau}{2-\tau}\right)\left(1-H_N{}^2\right)} \end{aligned}\right\} \quad (11)$$

While asymptotic limits may be used for the sake of simplicity, it is strongly advised to utilize exact time-varying limits for the practical implementation of the proposed chart. Time varying limits increase the control chart's capacity to promptly identify an off-target condition following the start of the $REWMA_N$ scheme.The time-varying limits of the proposed $REWMA_N$ chart can be alternatively written as

Alternatively, the time-varying limits for the proposed $REWMA_N$ chart can be rewritten as:

$$\left.\begin{aligned} LCL &= \beta_N d_{1N} \\ UCL &= \beta_N d_{2N} \end{aligned}\right\} \quad (12)$$

where $d_{1N} = H_N - K_N\sqrt{1-H_N{}^2}\sqrt{\left(\frac{\tau}{2-\tau}\right)\left[1-(1-\tau)^{2i}\right]}$, $d_{2N} = H_N + K_N\sqrt{1-H_N{}^2}\sqrt{\left(\frac{\tau}{2-\tau}\right)\left[1-(1-\tau)^{2i}\right]}$

$LCL = \min[LCL_l, LCL_u]$ and $UCL = \max[UCL_l, UCL_u]$.

Use of the suggested chart is predicated on the knowledge of the IC state parameter. However, in some circumstances, process parameters are frequently unavailable and must be estimated using phase-I samples. In case of unknown value of β_N (12) can be expressed as:

$$\left.\begin{aligned} LCL &= \bar{\beta}_N d_1 \\ UCL &= \bar{\beta}_N d_2 \end{aligned}\right\} \quad (13)$$

where $\bar{\beta}_N$ is computed from all T available sample subgroups each of size n. Using a Monte Carlo simulation with $\beta_N = [1, 2.5]$, the factor K_N is obtained, which corresponds to the estimated average run length when the process is in IC state(ARL_{0N}). The value of K_N, which determines the width of the control limits, is based on the ARL_{0N}. Table 1 presents the computed values of K_N for the proposed chart for various neutrosophic sample sizes, with the aim of achieving the desired ARL_{0N} value of [370, 400].

Doi: https://doi.org/10.54216/IJNS.230105
Received: October 05, 2023 Revised: November 01, 2023 Accepted: November 13, 2023

Table 1: Computed values of the factorK_N for $REWMA_N$ chart

Sample	ARL_0 ≈[370, 400]				
	τ=0.08	τ=0.15	τ=0.30	τ=0.60	τ=0.80
	K				
[2, 3]	[2.812, 2.796]	[2.845, 2.868]	[2.952,2.977]	[3.084,3.070]	[3.134,3.104]
[4, 5]	[2.723, 2.749]	[2.825, 2.855]	[2.939,2.977]	[3.029, 3.053]	[3.057, 3.061]
[6, 7]	[2.706, 2.735]	[2.823, 2.862]	[2.938, 2.984]	[3.014, 3.049]	[3.027, 3.058]
[8, 9]	[2.698, 2.724]	[2.832, 2.857]	[2.953, 2.976]	[3.013, 3.031]	[3.025, 3.042]
[10, 11]	[2.696, 2.726]	[2.829, 2.863]	[2.941, 2.974]	[3.004, 3.025]	[3.018, 3.039]
[12, 13]	[2.678, 2.725]	[2.815, 2.857]	[2.944, 2.974]	[3.008, 3.025]	[3.016, 3.036]
[14, 15]	[2.688, 2.725]	[2.826, 2.854]	[2.938, 2.964]	[3.009, 3.025]	[3.023, 3.043]

Additionally, Tables 2-4 presentd_{1N} and d_{1N} factors for different smoothing constants, including 0.15, 0.30 and 0.80.

Table 2: Neutrosophic factors d_{1N} and $d_{2N}$for the suggested chart at τ=0.15

Time index	Neutrosophic sample size					
	[2, 3]		[6, 7]		[14, 15]	
	d_{1N}	d_{2N}	d_{1N}	d_{2N}	d_{1N}	d_{2N}
1	[0.794, 0.838]	[1.081, 1.086]	[0.894, 0.902]	[1.063, 1.065]	[0.935, 0.937]	[1.047,1.048]
2	[0.749, 0.800]	[1.118, 1.131]	[0.867, 0.877]	[1.088,1.092]	[0.917, 0.919]	[1.064,1.065]
3	[0.721, 0.778]	[1.141, 1.158]	[0.851, 0.862]	[1.108, 1.103]	[0.907, 0.909]	[1.074, 1.076]
4	[0.704, 0.762]	[1.156, 1.176]	[0.841, 0.852]	[1.118, 1.112]	[0.900, 0.903]	[1.081, 1.082]
5	[0.692, 0.753]	[1.165,1.187]	[0.834, 0.846]	[1.119,1.125]	[0.895, 0.898]	[1.085, 1.087]
6	[0.684, 0.746]	[1.172, 1.196]	[0.829, 0.841]	[1.124,1.129]	[0.892,0.895]	[1.088, 1.090]
7	[0.678, 0.741]	[1.178, 1.202]	[0.826, 0.837]	[1.127, 1.133]	[0.890, 0.893]	[1.09, 1.093]
8	[0.674, 0.737]	[1.181, 1.206]	[0.823,0.835]	[1.129, 1.136]	[0.888, 0.891]	[1.092, 1.094]
9	[0.671, 0.735]	[1.184, 1.208]	[0.821, 0.834]	[1.131,1.137]	[0.887,0.890]	[1.093, 1.095]
10	[0.669, 0.733]	[1.185, 1.211]	[0.820, 0.833]	[1.132, 1.139,]	[0.886 , 0.889]	[1.094, 1.096]

Table 3: Neutrosophic factors $d_{1N}$and $d_{2N}$for the suggested chart at τ=0.30

Time index	Neutrosophic sample size					
	[2, 3]		[6, 7]		[14, 15]	
	d_{1N}	d_{2N}	d_{1N}	d_{2N}	d_{1N}	d_{2N}
1	[0.789, 0.833]	[1.085, 1.091]	[0.890, 0.899]	[1.066, 1.068]	[0.932, 0.935]	[1.049,1.050]
2	[0.742, 0.794]	[1.125, 1.138]	[0.863, 0.872]	[1.092, 1.096]	[0.914, 0.917]	[1.067, 1.068]
3	[0.714, 0.771]	[1.148, 1.166]	[0.846, 0.857]	[1.108, 1.113]	[0.903, 0.906]	[1.077, 1.079]
4	[0.695, 0.755]	[1.163, 1.185]	[0.835, 0.847]	[1.118, 1.123]	[0.896, 0.899]	[1.084, 1.086]
5	[0.683, 0.745]	[1.174,1.197]	[0.828, 0.840]	[1.125, 1.131]	[0.891, 0.894]	[1.089, 1.091]
6	[0.674, 0.738]	[1.181, 1.206]	[0.823, 0.835]	[1.130, 1.136]	[0.888, 0.891]	[1.092, 1.094]
7	[0.668, 0.733]	[1.186, 1.212]	[0.819, 0.832]	[1.133, 1.139]	[0.886,0.889]	[1.094, 1.097]
8	[0.664, 0.729]	[1.189, 1.216]	[0.817, 0.829]	[1.135, 1.142]	[0.884, 0.887]	[1.096, 1.098]
9	[0.661, 0.727]	[1.192, 1.219]	[0.815, 0.828]	[1.137, 1.144]	[0.883, 0.886]	[1.097, 1.099]
10	[0.659, 0.725]	[1.194, 1.221]	[0.814, 0.826]	[1.138, 1.145]	[0.882, 0.885]	[1.098, 1.100]

Table 4: Neutrosophic factors $d_{1N}$and$d_{2N}$for the suggested chart at τ=0.80

Time index	Neutrosophic sample size					
	[2, 3]		[6, 7]		[14, 15]	
	d_{1N}	d_{2N}	d_{1N}	d_{2N}	d_{1N}	d_{2N}
1	[0.780,0.828]	[1.091,1.100]	[0.888, 0.896]	[1.068, 1.071]	[0.931, 0.933]	[1.050, 1.051]

Doi: https://doi.org/10.54216/IJNS.230105
Received: October 05, 2023 Revised: November 01, 2023 Accepted: November 13, 2023

2	[0.729, 0.787]	[1.132, 1.151]	[0.859, 0.870]	[1.095, 1.100]	[0.912, 0.915]	[1.069, 1.070]
3	[0.700, 0.763]	[1.156, 1.180]	[0.842, 0.854]	[1.111, 1.117]	[0.901, 0.904]	[1.080, 1.081]
4	[0.680, 0.747]	[1.172, 1.200]	[0.831, 0.843]	[1.121, 1.128]	[0.893, 0.897]	[1.087, 1.089]
5	[0.667, 0.736]	[1.183, 1.213]	[0.823, 0.836]	[1.128, 1.135]	[0.888, 0.892]	[1.092, 1.094]
6	[0.658, 0.728]	[1.190, 1.222]	[0.818, 0.831]	[1.133, 1.141]	[0.885, 0.889]	[1.095, 1.097]
7	[0.652, 0.723]	[1.196, 1.228]	[0.815, 0.828]	[1.137, 1.144]	[0.883, 0.886]	[1.097, 1.100]
8	[0.647, 0.719]	[1.199, 1.233]	[0.812, 0.825]	[1.139, 1.147]	[0.881, 0.885]	[1.099, 1.101]
9	[0.644, 0.717]	[1.202, 1.236]	[0.810, 0.824]	[1.141, 1.149]	[0.880, 0.883]	[1.100, 1.103]
10	[0.641, 0.715]	[1.204, 1.239]	[0.809, 0.822]	[1.142, 1.150]	[0.879, 0.882]	[1.101, 1.103]

Tables 2–4 show that neutrosophic limits become narrower and converge to the constant limits as the time index increases.This is due to the fact that the factor $[1-(1-\tau)^{2i}]$in (11) goes to 1 as the sample size increases, leading to the eventual employment of the asymptotic limits at each sample point.Using the K_N factors from Table 1 can be used directly to construct proposed chart. However, having the factors$d_{1N}$and d_{1N}would make it much easier to construct the $REWMA_N$ control chart for the neutrosophic Rayleigh process.

4. Performance Evaluation

In this section, we will analyze and assess the measures that are used for measuring the performance of the suggested chart. Typically, control charts are used to ensure that processes run smoothly by providing early warning of any deterioration in process behavior. This enables technical staff to take corrective or preventive actions to mitigate any potential damage. Consequently, control chart users tend to focus on identifying declining performance. However, from a management perspective, it is equally important to be able to recognize situations where processes have been improved, whether through process stability, sub-process improvement, or learning effects. Therefore, the ability to identify OC situations is crucial for managers.Run length performance is a common metric used to assess the sensitivity of a control chart, which can be measured using various statistics, such as ARL_N, MRL_N, $SDRL_N$. Typically, ARL_N is used to evaluate the effectiveness of a control chart in detecting shifts. However, when examining the controls for a specific shift, $ARL_N$is usually calculated only for that shift. ARL_N can be further divided into two subcategories: ARL_{N0} and ARL_{N1}, representing the IC and OC states, respectively.For a control chart representing an IC process, we expect a large ARL_{N0} to avoid false alarms, whereas for a chart representing an OC process, we expect a shorter ARL_{N1} to detect changes in the process more quickly. When it comes to detecting changes in the underlying process parameter(s), a control chart is deemed superior to others if its $ARL_{N1}$is smaller than that of the other charts. In situations where the data has a skewed distribution, the MRL_N is also a recommended metric for assessing neutrosophic run length distribution (NRLD).In order to determine the run duration characteristics, a number of different methods can be employed, including Integral equations, Markov chains, and Monte Carlo simulation. Out of these three approaches, Monte Carlo simulation is considered to be the simplest. In this particular study, the run length characteristics of the proposed $REWMA_N$ control chart is calculated using Monte Carlo simulation. To evaluate the performance of the suggested control chart, a range of measures were simulated using Monte Carlo simulations. A simulation method was developed in R to model the behavior of the neutronic run length distribution, with 25000 iterations conducted for each shift. Tables 5-6 present the numerical findings for these performance indicators across various weighting constant values.In the case of an unstable process, parameter of the model, specifically β_{N0}, may shift to a new value denoted as$\Delta\beta_{N0}$, with the magnitude of this shift represented by the symbol Δ. A value of $\Delta = 1$ indicates that β_{N0} has not changed, while a value $\Delta > 1$ suggests that β_{N0} has increased, and a value $\Delta < 1$ suggests that β_{N0} has decreased. In our analysis, we have considered the situation where $\Delta > 1$ because an increase in variation is generally considered to be more problematic than a decrease in variance when monitoring a process.

Table 5: Performance of the $REWMA_N$ control chart at imprecise $ARL_{N0} = [370, 400]$

Shifted quantity	$\tau = 0.08$					
	$n = [2,3]$		$n = [6,7]$		$n = [12,13]$	
	ARL_N	MRL_N	ARL_N	MRL_N	ARL_N	MRL_N

Doi: https://doi.org/10.54216/IJNS.230105
Received: October 05, 2023 Revised: November 01, 2023 Accepted: November 13, 2023

1.00	[369.54, 400.31]	[255.8, 277.13]	[370.13, 400.59]	[256.21, 277.32]	[370.05, 400.04]	[256.15, 276.51]
1.05	[104.93, 122.61]	[72.38, 84.64]	[60.73, 62.2]	[41.75, 42.77]	[38.23, 38.48]	[26.15, 26.32]
1.08	[48.23, 58.40]	[33.08, 40.13]	[26.71, 27.73]	[18.17, 18.87]	[15.78, 16.4]	[10.59, 11.02]
1.10	[31.99, 38.76]	[21.83, 26.52]	[17.4, 18.24]	[11.71, 12.29]	[10.56, 10.98]	[7.26, 6.97]
1.12	[23.09, 27.57]	[15.66, 18.76]	[12.29, 13.02]	[8.17, 8.67]	[7.69, 7.89]	[4.98, 5.11]
1.14	[17.23, 21.00]	[14.21, 11.59]	[9.33, 9.85]	[6.11, 6.47]	[5.91, 6.02]	[3.74, 3.82]
1.16	[13.23, 15.83]	[8.82, 10.62]	[7.32, 7.78]	[4.72, 5.04]	[4.73, 4.74]	[2.92, 2.93]
1.50	[2.00, 2.28]	[1.00, 1.41]	[1.38, 1.47]	[1.00, 1.00]	[1.00, 1.00]	[1.00, 1.00]
1.80	[1.00, 1.45]	[1.00, 1.00]	[1.08, 1.11]	[1.00, 1.00]	[1.00, 1.00]	[1.00, 1.00]
2.00	[1.00, 1.26]	[1.00, 1.00]	[1.00, 1.00]	[1.00, 1.00]	[1.00, 1.00]	[1.00, 1.00]

Table 6: Performance of the $REWMA_N$ control chartat imprecise $ARL_{N0} = [370, 400]$

Shifted quantity	$\tau = 0.30$					
	$n = [2, 3]$		$n = [6, 7]$		$n = [12,13]$	
	ARL_N	MRL_N	ARL_N	MRL_N	ARL_N	MRL_N
1.00	[369.3, 400.92]	[255.63, 277.55]	[370.32, 399.93]	[256.34, 276.86]	[370.46, 400.34]	[256.44, 277.15]
1.05	[140.62, 146.67]	[97.12, 101.32]	[103.76, 104.14]	[71.57, 71.84]	[69.4, 71.35]	[47.76, 49.11]
1.08	[78.9, 89.19]	[54.34, 61.47]	[49.33, 50.92]	[33.85, 34.95]	[28.7, 29.53]	[19.54, 20.12]
1.10	[55.7, 65.56]	[38.26, 45.1]	[32.61, 33.95]	[22.26, 23.18]	[18.34, 19.07]	[12.36, 12.87]
1.12	[41.7, 50.38]	[28.56, 34.57]	[23.07, 24.39]	[15.64, 16.56]	[12.56, 13.1]	[8.35, 8.73]
1.14	[32.33, 39.64]	[22.06, 27.13]	[17.01, 17.96]	[11.44, 12.1]	[9.38, 9.85]	[6.15, 6.47]
1.16	[25.36, 31.98]	[17.23, 21.82]	[13.04, 13.97]	[8.69, 9.33]	[7.31, 7.67]	[4.71, 4.96]
1.50	[3.49, 4.49]	[2.05, 2.75]	[1.92, 2.14]	[1.00, 1.1]	[1.00, 1.00]	[1.00, 1.00]
1.80	[1.91, 2.39]	[1.00, 1.28]	[1.00, 1.33]	[1.00, 1.00]	[1.00, 1.00]	[1.00, 1.00]
2.00	[1.55, 1.9]	[1.00, 1.00]	[1.00, 1.00]	[1.00, 1.00]	[1.00, 1.00]	[1.00, 1.00]

Tables 5-6 present the NRLD characteristics for various sample sizes and shifts. When the process is in the IC state and for a given neutrosophic false alarm rate $\alpha_N = [\,0.0025,\ 0.0027]$, the average number of samples required to detect the first signal is [370, 400] across the sample sizes. However, in the case of a small shift with a vague sample size of $n = [2, 3]$, if the process experiences a 5% or 8% shift, the number of samples required is reduced to approximately [104.93, 122.61] and [48.23, 58.40], respectively. Overall, increasing the sample size improves the proposed chart's sensitivity to detect OC patterns. Additionally, results suggest that as the sample size increases for the same shift, the average number of samples required to detect a signal significantly decreases.

5. Simulation Study

This paper offers a novel extended design of the log-logistic distribution inside a neutrosophic framework, with the goal of more successfully handling fuzzy data with imprecise observations. The statistical features, moments, form coefficients, and survival characteristics of the suggested NLLD have been carefully examined. An estimation process is used to evaluate the performance of the anticipated neutrosophic parameters, assuring the accuracy and reliability of the model. The potential utility of NLLD in domains such as economics, engineering, survival analysis, and lifetime modeling is demonstrated by its practical implementation on a sample dataset of 128 bladder cancer patients. Overall, the NLLD is a promising strategy for dealing with uncertain and imprecise data that might be useful for academics and practitioners working with such data in a variety of disciplines. The effectiveness of the recommended substitution for the V_N-chart when smaller shifts are required to be detected is demonstrated in this section.Assuming that we want to monitor a

Doi: https://doi.org/10.54216/IJNS.230105
Received: October 05, 2023 Revised: November 01, 2023 Accepted: November 13, 2023

specific parameterβ_{N0} of the Rayleigh process in a particular application. For ease of understanding, it can be noted that the other distributional characteristics of the distribution will remain unchanged even if the target parameter undergoes a shift. The distribution of quality characteristic can be represented as R_{NO} prior to the shift in scale parameter and as R_{N1} after the observations from a RM_N that has an uncertain scale parameterβ_N= [0.8, 1].The plotted observations are depicted in Figure 2(a) on a Shewhart-type V_N-chart assuming ARL_0 =[370, 400] and n = [8, 9]. Likewise, Figure 2(b) illustrates the plotted thirty randomly selected observations on the proposed chart with a smoothing constant τ=0.30.

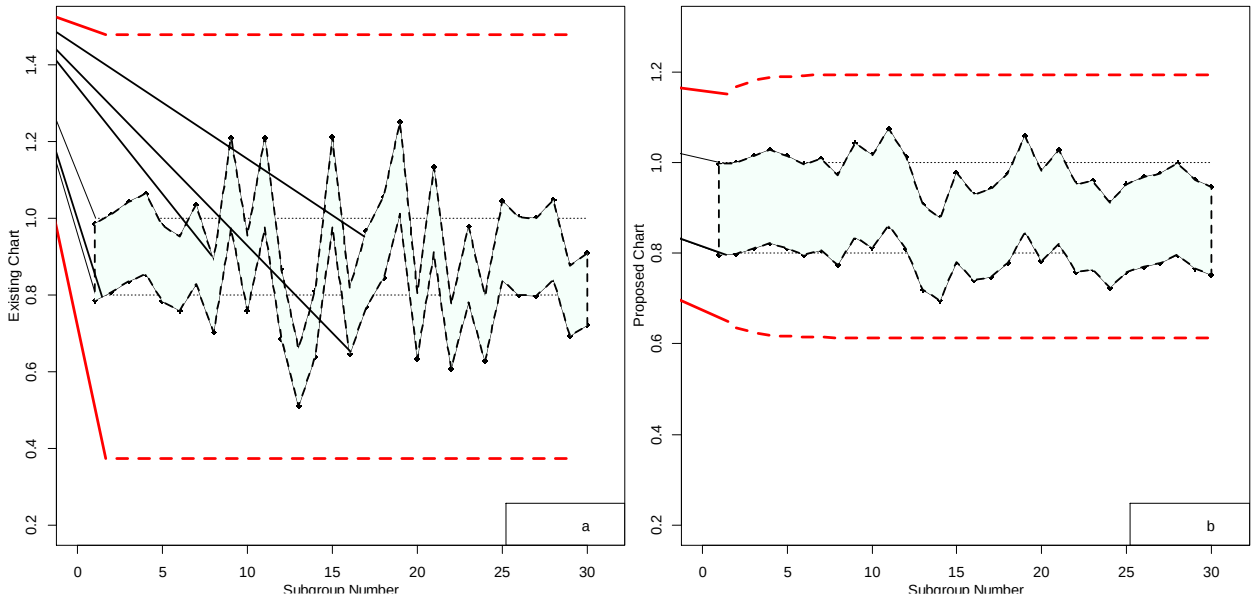

Figure 2: Control chart construction for simulated date with no change in the monitoring parameter

The fact that all of the displayed points in Figure 2 fall within the prescribed limits of both existing and proposed chart, indicates that the underlying process is under statistical control. These thirty subgroups may be considered as sample date collected from R_{NO} distribution. Now let us assume that twenty observations are chosen from R_{NO} process, and the last ten observations are selected from the process R_{N1}, whereβ_N= [1, 1.25], indicating a 25% increase in the scale parameter of the R_{NO}distribution. All thirty observations are displayed on both charts in Figure 3.

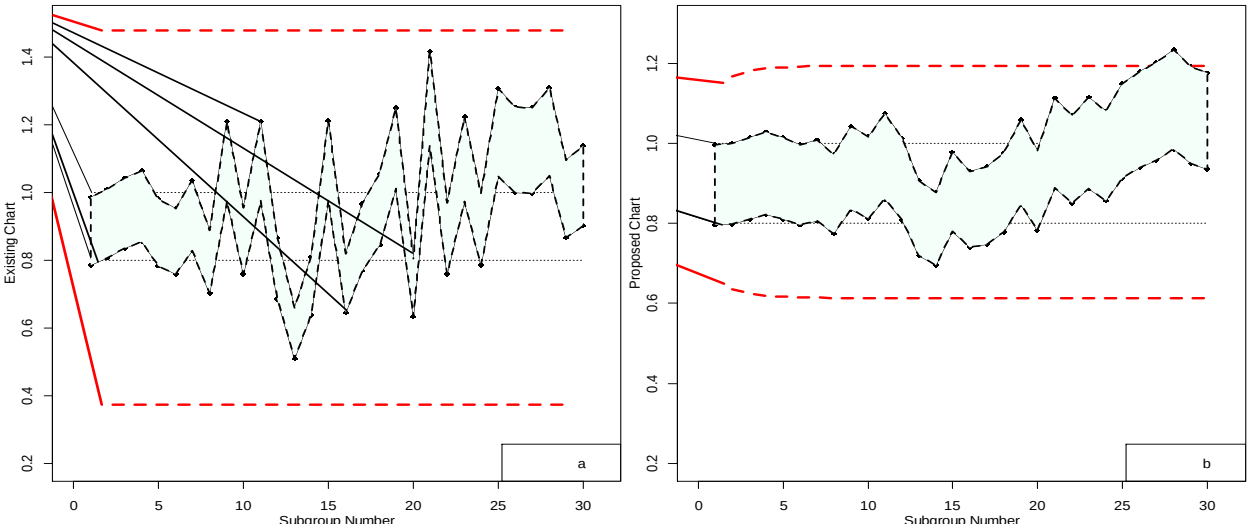

Figure 3: Control chart construction for a simulated date with a 25% upward shift in the monitoring parameter

Doi: https://doi.org/10.54216/IJNS.230105
Received: October 05, 2023 Revised: November 01, 2023 Accepted: November 13, 2023

Figure 3(a) demonstrates that none of the plotted points falls beyond the control bounds, indicating a lack of strong evidence suggesting that the process is out of control. Thus the existing chart is not sensitive to undergo smaller magnitude shifts in the target parameter.In contrast, Figure 3(b) illustrates a developed upward drift in plotted data after the 20th sample, indicating the process is in an OC state. Thus the proposed chart is a suitable alternative when diagnosing persistent shifts is crucial.

6. Comparative analysis

This section aims to compare the suggested $REWMA_N$ control chart with the previously developed V_N chart. Power curves, a well-known method of evaluating the efficacy of control charts, are used to examine the efficiency of the suggested chart. Within the context of a control chart applications power indicates the likelihood of either rejecting a batch of inferior items or allowing a process to continue while reaching the required quality standard for a certain characteristic. A control chart that exhibits higher sensitivity towards detecting specific shifts in the process is deemed to be more efficient. The power of the proposed control chart was determined by selecting constants from Table 1 for sample sizes $n = [2, 3]$ and $n = [6, 7]$at τ= 0.30. Total of 25000 simulation runs from the RM_N with β_{N0}= [0.8, 1] at a fixed value of$ARL_{N0} = [370, 400]$are performed. A simulation program was developed using R software to assess the power of both charts, and the resulting power values are displayed in Figure 3.

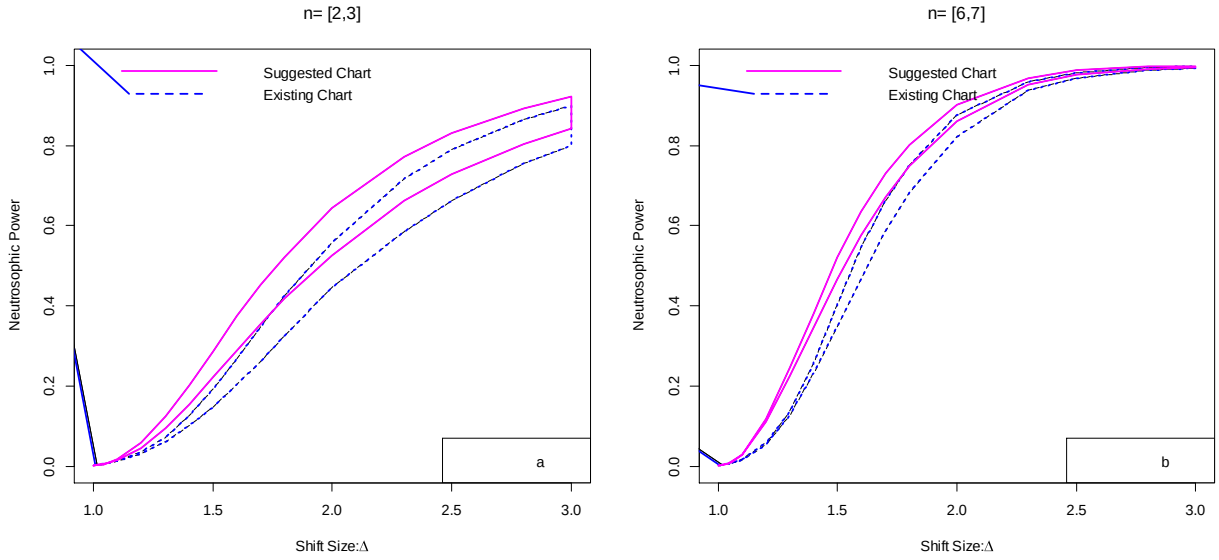

Figure 3: Power comparisons of the $REWMA_N$ control chart with the existing V_N chart

As shown in Figure 3, when ARL_{N0} is fixed, the power probabilities tend to rise as the shift constant increases. At shift quantity equal to one, both charts behave similarly and offer power that is closer to the value of that is assumed, i.e., $\alpha = [0.025, 0.027]$, and this results in $ARL_{N0} = [370, 400]$. However, the power of the proposed control chart is greater than that of the existing chart because the lower and upper control limits of the proposed $REWMA_N$ chart is higher than those of the existing V_N chart. Therefore, the $REWMA_N$ chart consistently performs better than the V_N chart for minor changes in the scale parameter of the Rayleigh process.

7. Real World Data Application

In this section, we illustrate the application of the proposed chart specifically designed for the RM_N using real-world dataset of daily average wind speed (in Km/Hr) reported at Elanora Heights located in Sydney, Australia in the month of November 2007 [36]. For additional details about the dataset, refer to the work [37]. In reference [37], the utilization of an expanded one-parameter Rayleigh

Doi: https://doi.org/10.54216/IJNS.230105
Received: October 05, 2023 Revised: November 01, 2023 Accepted: November 13, 2023

distribution for modeling the data was elucidated and examined. It was concluded that the data is a good fit for the extended Rayleigh distribution. Nonetheless, it is possible to assess the suitability of the standard one-parameter Rayleigh distribution. Figure 3 displays the fittingprobability plots of the Rayleigh (red lines) model with respect to the data.

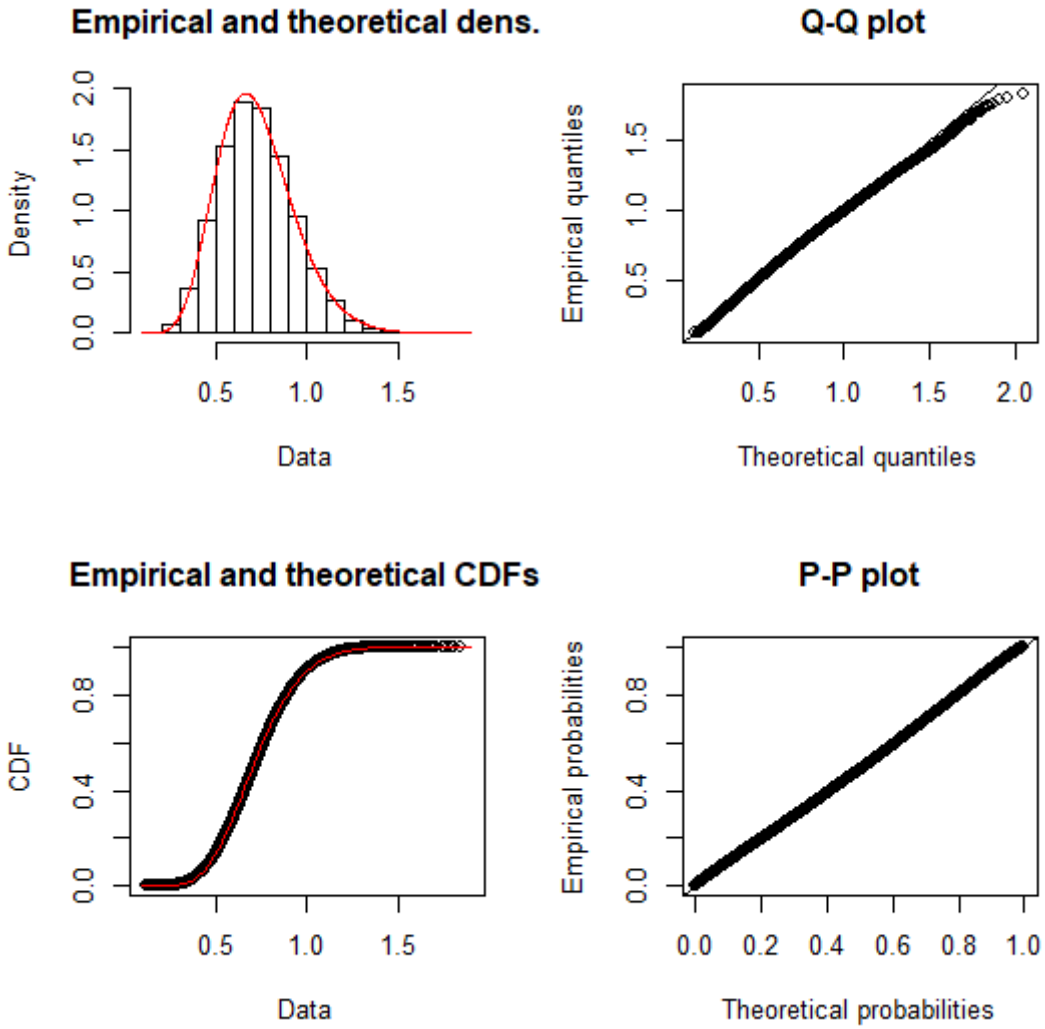

Figure 4: Fitting plots of the Rayleigh model on daily average wind speed dataset

Based on the probability plots in Figure 4, it can be inferred that the Rayleigh distribution is a potential candidate for the underlying distribution of the data. The validity of the model can be formally tested using various statistical tests, such as the Kolmogorov-Smirnov (KS) test. In the case of the wind speed dataset data, the KS test yielded a distance of 0.209 and a p-value of 0.620, which also suggests that the Rayleigh distribution is a suitable candidate for the data. Hence, the dataset can be employed for constructing the $REWMA_N$ chart. The method described by Khan et al. [24] is utilized to create Neutrosophic data for the purpose of conceptualizing the $REWMA_N$ control chart. However, it should be noted that the original data source provides precise numerical values. In order to establish the proposed control chart, the data is divided into subgroups of size 3, resulting in a total of 10 subgroups being created. The uncertain dataset along the plotting statistic, are shown in Table 7.

Doi: https://doi.org/10.54216/IJNS.230105
Received: October 05, 2023 Revised: November 01, 2023 Accepted: November 13, 2023

Table 7: Indeterminate average wind speed dataset along with computed statistic

Sample Number	Observations			$\hat{V}_{SQR}$	Bounds for proposed chart	
	I	II	III		LCL	UCL
1	[2.20, 2.79]	[3.07, 4.96]	[2.02, 2.24]	[1.75, 2.50]	1.87	4.46
2	[3.91, 4.91]	[7.48, 8.29]	[4.38, 4.92]	[3.88, 4.42]	1.73	4.67
3	[3.62, 4.38]	[3.29, 4.42]	[2.07, 3.97]	[2.17, 3.01]	1.66	4.75
4	[2.54, 3.87]	[4.51, 4.70]	[4.70, 6.20]	[2.85, 3.55]	1.63	4.80
5	[4.10, 6.08]	[3.86, 5.22]	[3.58, 4.22]	[2.72, 3.70]	1.62	4.81
6	[2.37, 3.72]	[4.51, 5.26]	[3.49, 5.32]	[2.52,3.41]	1.61	4.82
7	[6.79, 7.74]	[7.69, 11.88]	[4.76, 5.65]	[4.62, 6.23]	1.61	4.82
8	[1.84, 4.34]	[3.94, 4.38]	[2.83, 5.50]	[2.12, 3.37]	1.61	4.82
9	[1.69, 4.77]	[2.86, 4.28]	[2.38, 4.50]	[1.67, 3.20]	1.60	4.82
10	[3.47, 5.52]	[1.64, 4.18]	[3.75, 4.84]	[2.19, 3.45]	1.60	4.82

Once it has been established that the Rayleigh distribution is an acceptable fit for the data, the next step would be to determine the appropriate limits for the proposed chart.Table 1 shows that when the sample size is crisp value i.e., $n = [3, 3]$, the resulting K_N values are [2.977, 2.977] at $\tau = 0.30$. The average value of the plotted statistic $\bar{\beta}_N = [2.65, 3.68]$ is computed from all 10 available sample subgroups in Table 7. The upper and lower limits of the $REWMA_N$ chart is calculated using these values and is presented in the last two columns of Table 7. It is important to note that each limit represents the minimum and maximum values of the neutrosophic intervals. Figure 5 displays the plotted statistic along with the limits constructed using Eq. (14).

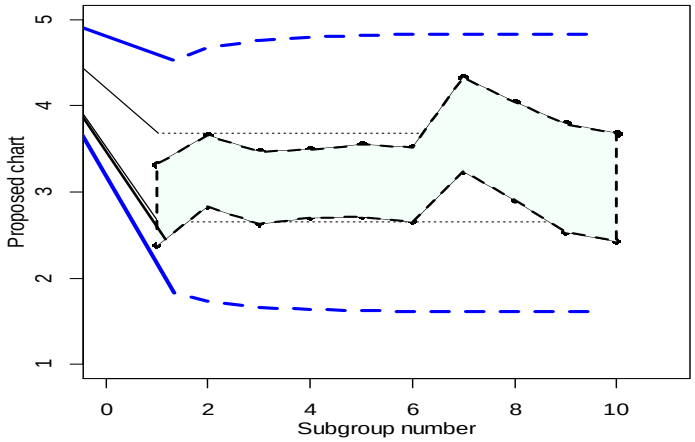

Figure 5: The $REWMA_N$ chart for the daily wind speed data

Based on Figure 5, it appears that the uncertain wind speed data falls within the constructed limits, indicating that it is not significantly deviating from the expected values. Therefore, specific quality control measures do not need to be implemented to flag alerts to users of the data.

8. Conclusions

The study introduces an improved method called the $REWMA_N$ chart, which is designed to enhance the detection capability of the traditional V_{NR} chart.The proposed chart is capable of handling vague, indeterminate, and fuzzy data situations, making it suitable for a wide range of applications.The key features of the proposed chart are discussed, and its performance is evaluated by analyzing the designated limits and charting parameters for different sample sizes. This study has also established the neutrosophic parameters of the $REWMA_N$ chart and its performance metrics, such asARL_N and PC_N. Monte Carlo simulations have been conducted to compare the suggested scheme with the existing model. Results indicate that the proposed chart outperforms the competing design in detecting shift

Doi: https://doi.org/10.54216/IJNS.230105
Received: October 05, 2023 Revised: November 01, 2023 Accepted: November 13, 2023

amounts.Performance evaluation demonstrates that the $REWMA_N$the chart is highly sensitive to smaller shifts in the scaling parameter of the RM_N.Finally, the study has provided a charting structure for the proposed design using daily average wind speed data, which can be used as a practical implementation guideline for real-world applications.

Acknowledgement: The authors extend their appreciation to Prince Sattam Bin Abdulaziz University for funding this research work through the project number (PSAU/2023/01/24852).
Conflicts of Interest: The authors declare no conflict of interest.

References

[1] Khaliq, Q. U., Riaz, M., & Arshad, I. A. (2021). On the performance of median-based Tukey and Tukey-EWMA charts under rational subgrouping. Science Iran, 28(1), 547-556, 2021

[2] Park, K., Jung, D., & Kim, J. M. (2020). Control charts based on randomized quantile residuals. Applied Stochastic Models in Business and Industry, 36(4), 716-729, 2020.

[3] Montgomery, D. Introduction to Statistical Quality Control, Sixth Edition. John Wiley & Sons, Inc, 2009.

[4] Zaka, A., Jabeen, R., & Khan, K. I. Control charts for the shape parameter of skewed distribution. Intelligent Automation & Soft Computing, 30(3), 2021

[5] Javaid, A., Noor-ul-Amin, M., & Hanif, M. Performance of Max-EWMA control chart for joint monitoring of mean and variance with measurement error. Communications in Statistics - Simulation and Computation, 52(1), 4-40, 2023

[6] Hussain, S., Wang, X., Ahmad, S., & Riaz, M. On a class of mixed EWMA-CUSUM median control charts for process monitoring. Quality and Reliability Engineering International, 36(3), 2020.

[7] Erginel, N., & Şentürk, S. Fuzzy EWMA and fuzzy CUSUM control charts. Studies in Fuzziness and Soft Computing, 343, 95-281, 2016.

[8] Nawaz, M. S., Azam, M., & Aslam, M. EWMA and DEWMA repetitive control charts under non-normal processes. Journal of Applied Statistics, 48(1), 4-40, 2021.

[9] Pedro M. García,Gilberto F. Castro,Inelda A. Martillo,Maikel Y. L. Vázquez, Redesign of a drone (UAV) to obtain high flight autonomy, used in the analysis of Pitahaya crops based on neutrosophic control, International Journal of Neutrosophic Science, Vol. 19 , No. 3 , (2022) : 53-62 (Doi : https://doi.org/10.54216/IJNS.190306)

[10] Best, D. J., Rayner, J. C. W., & Thas, O. Easily applied tests of fit for the Rayleigh distribution. Sankhya B, 72(2), 254-263, 2010

[11] Abbasi, S. A., Riaz, M., Miller, A., Ahmad, S., & Nazir, H. Z. EWMA Dispersion Control Charts for Normal and Non-normal Processes. Quality and Reliability Engineering International, 31(8), 1691-1704, 2015.

[12] Derya, K., & Canan, H. G. Control charts for skewed distributions: Weibull, gamma, and lognormal. Advances in Methodology and Statistics, 9(2), 95-106, 2012.

[13] Santiago, E., & Smith, J. Control charts based on the exponential distribution: Adapting runs rules for the t chart. Quality Engineering, 25(2), 85-96, 2013

[14] Rosaiah, K., Rao, B. S., Reddy, J. P., & Chinnamamba, C. Variable control charts for Gumbel distribution based on percentiles. Journal of Computational Mathematics and Sciences, 9(12), 1890-1897, 2018.

[15] Hossain, M. P., Omar, M. H., & Riaz, M. (2017). New V control chart for the Maxwell distribution. Journal of Statistical Computation and Simulation, 87(3), 594-606.

[16] Basant Sameh, Mahmoud Elshabrawy, Seasonal Autoregressive Integrated Moving Average for Climate Change Time Series Forecasting, American Journal of Business and Operations Research, Vol. 8 , No. 2 , (2023) : 25-35 (Doi : https://doi.org/10.54216/AJBOR.080203)

Doi: https://doi.org/10.54216/IJNS.230105
Received: October 05, 2023 Revised: November 01, 2023 Accepted: November 13, 2023

[17] Hussein Alkattan, Sanjar Abdullaev, El-Sayed M. El-Kenawy, The «Climate in Weathers» Approach to Processing of Meteorological Series in Mesopotamia: Assessment of Climate Similarity and Climate Change using Data Mining, Journal of Intelligent Systems and Internet of Things, Vol. 10 , No. 1 , (2023) : 48-65 (Doi : https://doi.org/10.54216/JISIoT.100104)

[18] Hossain, M. P., Omar, M. H., Riaz, M., & Arafat, S. Y. (2020). On designing a new control chart for Rayleigh distributed processes with an application to monitor glass fiber strength. Communications in Statistics - Simulation and Computation, 1-17.

[19] Khan, Z., Gulistan, M., Kadry, S., Chu, Y., & Lane-Krebs, K. (2020). On scale parameter monitoring of the Rayleigh distributed data using a new design. IEEE Access, 8, 188390-188400.

[20] Alduais, F. S., & Khan, Z. EWMA Control Chart for Rayleigh Process With Engineering Applications. IEEE Access, 11, 10196-10206, 2023.

[21] Aslam, M. Attribute Control Chart Using the Repetitive Sampling Under Neutrosophic System. IEEE Access, 7, 15367-15374, 2019.

[22] Aslam, M., Khan, N., & Khan, M. Z. Monitoring the variability in the process using neutrosophic statistical interval method. Symmetry, 10(11), 562, 2018

[23] Aslam, M., & Arif, O. Testing of grouped product for the Weibull distribution using neutrosophic statistics. Symmetry (Basel), 10(9), 403, 2018

[24] Khan, Z., Gulistan, M., Hashim, R., Yaqoob, N., & Chammam, W. A New Dispersion Control Chart for Handling the Neutrosophic Data. IEEE Access, 8, 96006-96015, 2020.

[25] Khan, Z., Gulistan, M., Rosaiah, K., & Park, C. Neutrosophic Rayleigh Model with Some Basic Characteristics and Engineering Applications. IEEE Access, 9, 71277-71283, 2021.

[26] Atalik, G., & Senturk, S. (2022). Intuitionistic fuzzy c control charts based on intuitionistic fuzzy ranking method for TIFNs. Soft Computing, 26(21), 11403-11407, 2022

[27] Khan, M. Z., Khan, M. F., Aslam, M., & Mughal, A. R. A study on average run length of fuzzy EWMA control chart. Soft Computing, 26(18), 9117-9124, 2022.

[28] Smarandache, F. Neutrosophic logic - a generalization of the intuitionistic fuzzy logic. In Multispace & Multistructure (100 Collected Papers of Science), Vol. 4, pp. 396, 2010.

[29] Smarandache, F., Broumi, S., Singh, P. K., Liu, C. F., Rao, V. V., Yang, H. L., Patrascu, I., & Elhassouny, A. Introduction to neutrosophy and neutrosophic environment. In Neutrosophic Set in Medical Image Analysis (pp. 3-29). Academic Press, 2019.

[30] Smarandache, F. L. Introduction to Neutrosophic Statistics. Sitech and Education Publisher, Craiova, Romania-Educational Publisher, Columbus, Ohio, USA, p. 123, 2014.

[31] Broumi, S., Sundareswaran, R., Shanmugapriya, M., Bakali, A., & Talea, M. Theory and Applications of Fermatean Neutrosophic Graphs. Neutrosophic Sets and Systems, 50, 248-286. 2022.

[32] Broumi, S., Sundareswaran, R., Shanmugapriya, M. ., Nordo, G. ., Talea, M. ., Bakali, A., & Smarandache, F. Interval- valued fermatean neutrosophic graphs. Decision Making

[33] Aslam, M., & Raza, M. A. Design of New Sampling Plans for Multiple Manufacturing Lines Under Uncertainty. International Journal of Fuzzy Systems, 21(3), 978-992, 2019.

[34] Shafqat, A., Aslam, M., Saleem, M., & Abbas, Z. The new neutrosophic double and triple exponentially weighted moving average control charts. Computers & Mathematics with Applications, 129(1), 373-391, 2021.

[35] Kundu D, Raqab M. Z. Generalized Rayleigh distribution: different methods of estimations. Computational Statistics & Data Analysis, 49(1), 187-200, 2005

[36] Jahanshahi S. M. A., Habibirad A, Fakoor V. Some new goodness-of-fit tests for Rayleigh distribution. Pakistan Journal of Statistics and Operational Research, 16(2), 305-315, 2020

[37] Best D. J, Rayner J. C. W., Thas O. Easily applied tests of fit for the Rayleigh distribution. Sankhya B, 72(2):254-263, 2010

Doi: https://doi.org/10.54216/IJNS.230105
Received: October 05, 2023 Revised: November 01, 2023 Accepted: November 13, 2023